

Study of near-surface models for large-eddy simulations of a neutrally stratified atmospheric boundary layer

Inanc Senocak · Andrew S. Ackerman ·
Michael P. Kirkpatrick · David E. Stevens ·
Nagi N. Mansour

Received: 19 July 2006 / Accepted: 7 March 2007 / Published online: 27 April 2007
© Springer Science+Business Media B.V. 2007

Abstract In large-eddy simulations (LES) of the atmospheric boundary layer (ABL), near-surface models are often used to supplement subgrid-scale (SGS) turbulent stresses when a major fraction of the energetic scales within the surface layer cannot be resolved with the temporal and spatial resolution at hand. In this study, we investigate the performance of both dynamic and non-dynamic eddy viscosity models coupled with near-surface models in simulations of a neutrally stratified ABL. Two near-surface models that are commonly used in LES of the atmospheric boundary layer are considered. Additionally, a hybrid Reynolds-averaged/LES eddy viscosity model is presented, which uses Prandtl's mixing length model in the vicinity of the surface, and blends in with the dynamic Smagorinsky model away from the surface. Present simulations show that significant portions of the modelled turbulent stresses are generated by the near-surface models, and they play a dominant role in capturing the expected logarithmic wind profile. Visualizations of the instantaneous vorticity

I. Senocak
Center for Turbulence Research, NASA-Ames/Stanford University,
Stanford, CA 94305, USA

I. Senocak (✉)
Los Alamos National Laboratory Mail stop k575, P.O. Box 1663,
Los Alamos, NM 87545, USA
e-mail: senocak@lanl.gov

A. S. Ackerman
NASA Goddard Institute for Space Studies, New York, NY 10025, USA

M. P. Kirkpatrick
School of Aerospace, Mechanical and Mechatronic Engineering,
University of Sydney, Sydney 2006, Australia

D. E. Stevens
Lawrence Livermore National Laboratory, Livermore, CA 94550, USA

N. N. Mansour
NASA Ames Research Center, Moffett Field, CA 94035, USA

field reveal that flow structures in the vicinity of the surface depend on the choice of the near-surface model. Among the three near-surface models studied, the hybrid eddy viscosity model gives the closest agreement with the logarithmic wind profile in the surface layer. It is also observed that high levels of resolved turbulence stresses can be maintained with the so-called canopy stress model while producing good agreement with the logarithmic wind profile.

Keywords Atmospheric boundary layer · Dynamic models · Large-eddy simulations · Near-surface models

1 Introduction

Large-eddy simulation (LES) is a widely used technique in atmospheric research, partly due to the difficulties associated with obtaining detailed information on the small-scale turbulent structure of the atmosphere through direct observational measurements (Stevens and Lenschow, 2001). In LES, large unsteady three-dimensional structures are resolved, and small structures that are not resolved on the computational grid are modelled. A filtering operation is applied to distinguish between resolved and unresolved scales. Unresolved motions are assumed to be universal, and simple subgrid-scale (SGS) models should be sufficient to parameterize them, provided that a major fraction of the energetic scales are resolved by the spatial and temporal resolutions (Sagaut 2002). These resolution requirements become computationally not feasible, however, in proximity to the surface.

As the surface is approached, anisotropy in turbulence structure increases, and the length scale of the flow structures diminishes rapidly, requiring too fine a spatial and temporal resolution to numerically resolve a large fraction of the energetic scales. Hence, sufficiently resolved LES of surface-bounded high Reynolds number flows are prohibitively expensive in terms of computational resources. Additionally, roughness of the surface underlying the atmospheric boundary layer and modelling of sensible and latent heat fluxes over complex structures cannot be addressed by higher resolution in the vicinity of the surface. These surface complexities contribute significantly to the mean and higher-order properties of the flow, and need to be parameterized accurately.

In modelling the surface, no-slip boundary conditions are not applied directly, because the implied stress would be unrealistically exaggerated on a coarse mesh. A simple surface model that has long been adopted in atmospheric boundary-layer simulations assumes that a logarithmic wind profile exists within the surface layer, and stresses are imposed as boundary conditions at the surface (e.g. Schumann 1975; Moeng 1984). Cabot et al. (1999) showed that such models are not effective for high Reynolds number LES with numerical resolutions that are considered as “coarse/poor” with respect to resolving a large portion of the energetic scales. Cabot (1997) indicated that providing accurate mean surface stresses is not sufficient to overcome these deficiencies. He suggested that, given a coarse numerical resolution, typical SGS models used in LES cannot adequately predict Reynolds stresses in the near-surface region. Sullivan et al. (2003) investigated the structure of the SGS turbulent motions in the atmospheric surface layer using field data and attributed the difficulty of performing LES with a standard Smagorinsky model to the increased dominance of SGS motions and their departure from the classical inertial-range turbulence.

Boundary-layer approximations have been proposed to extend the application of LES with surface models to separating flows (Balaras et al. 1996 Cabot and Moin 2000). In this approach, a simplified set of turbulent boundary-layer equations, adopting a Reynolds-

averaged Navier-Stokes (RANS) type eddy viscosity, are solved on an embedded mesh near the surface. The surface stress is then calculated from the computed velocity profile. Within this framework, [Wang and Moin \(1992\)](#) used a dynamically adjusted mixing length eddy viscosity, and showed predictions that are in good agreement with experimental data.

In atmospheric boundary-layer simulations, a common practice to improve predictions near the surface is to employ LES models away from the surface, and make a transition towards ensemble-averaged (RANS) models as the surface is approached. This approach has been implemented through different formulations. For instance, [Sullivan et al. \(1994\)](#) proposed an eddy viscosity model in which the so-called isotropy factor controls the transition from LES to a RANS type simulation, and accounts for the anisotropy effects at the same time. [Wyngaard et al. \(1998\)](#) analyzed LES data with various resolutions, and highlighted the importance of compatibility of the surface boundary conditions with SGS models for better predictions. Within the context of the classical Smagorinsky SGS model, [Mason and Thomson \(1992\)](#) used a modified length scale proposed by [Mason and Callen \(1986\)](#) that is a function of both the LES subgrid length scale and the distance from the surface. [Mason and Thomson \(1992\)](#) also proposed an optional stochastic backscatter model, which introduces random SGS stresses to improve the matching between different length scales. [Hobson et al. \(1999\)](#) did a detailed test study of the Mason–Thomson model with and without the stochastic backscatter model. They showed that the stochastic backscatter model improves the wind speed profile in the length scale matching region, and produces results with very little resolution dependence.

Traditionally, canopy models have been adopted to parameterize the effect of flow within a vegetative canopy layer. [Brown et al. \(2001\)](#) suggested using a canopy stress model with the aim of overcoming the numerical under-resolution issues related to LES modelling of rough surfaces with no vegetation. In their approach, instead of direct modification of the eddy viscosity or the length scale, additional turbulent stresses are added to the turbulent stresses modelled by the SGS model. [Cederwall \(2002\)](#), [Chow et al. \(2005\)](#) and [Kirkpatrick et al. \(2006\)](#) adapted the canopy stress model of [Brown et al. \(2001\)](#) for atmospheric boundary layer simulations, and reported improved predictions of the expected wind profile within the surface layer.

[Porte-Agel et al. \(2000\)](#) explained the inconsistency of the assumption of scale invariance in the dynamic Smagorinsky model when the filter scales fall outside of the inertial sub-range, and developed a scale-dependent dynamic model for the neutral ABL. Near the surface, the scale invariant assumption of the dynamic procedure is relaxed, and the length scale becomes comparable to the distance to the surface. The scale-dependent dynamic model gave better predictions of the logarithmic wind profile than both the dynamic Smagorinsky and the original (non-dynamic) Smagorinsky model.

Apart from the deficiencies of LES SGS models near the surface, most SGS models have prescribed parameters that need tuning for different problems in order to improve the predictions. For large scale problems with complex geometry, it is desirable to minimize or avoid the need for tuning these parameters. To address this issue, [Germano et al. \(1991\)](#) introduced the dynamic procedure for SGS models. In the dynamic procedure, SGS model parameters are computed based on the information available in the resolved flow field. [Germano et al. \(1991\)](#) applied the dynamic procedure to compute the model parameter in the original Smagorinsky model ([Smagorinsky 1963](#)). The dynamic procedure is not limited to the Smagorinsky model, and it has been extended to other SGS models ([Ghosal et al. 1995](#)). Dynamic SGS models have found wide and successful use in complex engineering flow problems, and their application to atmospheric boundary-layer flows has received increased attention in recent years. To our knowledge, [Bohnert \(1993\)](#) is the earliest study adopting the dynamic procedure for

LES of the atmospheric boundary layer. Bohnert's study of a moist low Reynolds number Ekman layer used relatively simple parameterizations for radiation and cloud physics, and found that the dynamic Smagorinsky model gave similar results to those obtained using a tuned non-dynamic SGS model. Kirkpatrick et al. (2006) have further extended the dynamic Smagorinsky model for a realistic stratocumulus-topped boundary layer, taking into account buoyancy and stratification effects and have reported improved agreement with observations. The dynamic procedure has also been used in LES of stable and clear ABLs by Cederwall (2002), and for a neutrally stratified ABL by Chow et al. (2005). All these studies have demonstrated that there are considerable advantages in utilizing dynamic SGS models for atmospheric flow simulations. It should be emphasized that the dynamic Smagorinsky model alone does not address the poor performance of SGS models within the surface layer of the ABL. As shown by Porte-Agel et al. (2000), underlying assumptions concerning the length scale used in the SGS model can be relaxed to derive a scale-dependent dynamic SGS model. Alternatively, near-surface models can be used to supplement dynamic SGS in the poorly resolved region close to the surface.

In what follows, we study two near-surface models that have found use in LES of the atmospheric boundary layer (the Mason–Thomson model without backscatter and the canopy stress model). Following the two-part eddy viscosity approach of Sullivan et al. (1994), we also present a hybrid RANS/LES eddy viscosity model that adopts Prandtl's mixing length model (Prandtl 1925) close to the surface, and blends with the dynamic Smagorinsky model (Germano et al. 1991) away from the surface. Our goal is to investigate the performance of these near-surface models in large-eddy simulations of a neutrally stratified atmospheric boundary layer.

2 Governing equations

The governing equations for LES of a neutrally stratified incompressible atmospheric boundary layer are the filtered Navier-Stokes equations

$$\frac{\partial \bar{u}_i}{\partial x_i} = 0, \quad (1a)$$

$$\frac{\partial \bar{u}_i}{\partial t} + \frac{\partial (\bar{u}_i \bar{u}_j)}{\partial x_j} = -\frac{\partial \bar{p}}{\partial x_i} - \epsilon_{ijk} f_j (\bar{u}_k - u_k^g) - \frac{\partial \tau_{ij}}{\partial x_j}, \quad (1b)$$

where turbulent stresses are defined as $\tau_{ij} = \overline{u_i u_j} - \bar{u}_i \bar{u}_j$, f_j is the Coriolis parameter, ϵ_{ijk} is the permutation tensor, u_k^g is the geostrophic wind, \bar{u} and \bar{p} are the filtered velocity and filtered non-hydrostatic component of pressure, respectively.

In all simulations, we use periodic lateral boundary conditions, and impose a stress-free condition on the upper boundary. At the lower boundary, the vertical component of velocity is set to zero, and horizontal components of the turbulent stresses are defined based on the mean logarithmic wind profile assumption as follows (Moeng 1984)

$$\tau_{i3} = -\left(\frac{\kappa}{\ln \frac{z_1}{z_0}}\right)^2 |\bar{\mathbf{u}}| \bar{u}_i, \quad (2)$$

where κ is the von Karman constant (we assume a value of 0.41), and z_1 and u_i are the altitude and the horizontal wind components of the first grid point above the surface, respectively. The surface roughness is taken into account through the roughness length z_0 .

3 Subgrid-scale turbulence modelling

Turbulent stresses that appear in Eq. (1b) can be modelled based on eddy viscosity assumption. The model of Smagorinsky (1963) is a popular eddy viscosity approach, which represents turbulent stresses as

$$\tau_{ij} = -2(C_s l)^2 |\bar{S}| \bar{S}_{ij}. \quad (3)$$

In the above equation $|\bar{S}|$ is the magnitude of the filtered strain rate tensor defined as

$$|\bar{S}| = \sqrt{2\bar{S}_{ij}\bar{S}_{ij}}, \quad (4a)$$

$$\bar{S}_{ij} = \frac{1}{2} \left(\frac{\partial \bar{u}_i}{\partial x_j} + \frac{\partial \bar{u}_j}{\partial x_i} \right). \quad (4b)$$

We define the filter width $\Delta = (dx \cdot dy \cdot dz)^{1/3}$ as the length scale l in the eddy viscosity definition given by Eq. 3, where dx , dy and dz are the dimensions of the grid cell. In the original Smagorinsky model, the dimensionless parameter C_s is a prescribed constant, whereas in the dynamic Smagorinsky model (Germano et al. 1991), this parameter is often written as $C = C_s^2$, and computed dynamically, making it a function of space and time. In the original Smagorinsky model, which is only adopted along with the Mason–Thomson near-surface model, we use $C_s = 0.18$.

The dynamic Smagorinsky model involves filters of different sizes. In addition to the grid filter, which is implicit in the finite difference computations, an explicit spatial test filter is introduced. A spatial box filter is used in the present computations. The subgrid-scale stress tensor based on the grid and test filters is written respectively as

$$\tau_{ij} = \overline{u_i u_j} - \bar{u}_i \bar{u}_j, \quad (5a)$$

$$T_{ij} = \widehat{\overline{u_i u_j}} - \hat{\bar{u}}_i \hat{\bar{u}}_j, \quad (5b)$$

where the symbols overbar and the hat represent the grid and test filtering operations, respectively. Applying the test filter to τ_{ij} and subtracting it from T_{ij} yields the following identity (Germano et al. 1991)

$$L_{ij} = T_{ij} - \hat{\tau}_{ij} = \widehat{\overline{u_i u_j}} - \hat{\bar{u}}_i \hat{\bar{u}}_j. \quad (6)$$

The significance of this identity is that it can be computed from the resolved flow. Germano et al. (1991) have utilized this identity to dynamically compute the coefficient of the Smagorinsky model $C = C_s^2$ as follows:

$$L_{ij} - \frac{1}{3} \delta_{ij} L_{kk} = \alpha_{ij} C - \widehat{\beta_{ij} C}, \quad (7)$$

where

$$\alpha_{ij} = -2\widehat{\Delta^2 \widehat{\bar{S}}_{ij}}, \quad (8a)$$

$$\beta_{ij} = -2\Delta^2 \bar{S}_{ij}. \quad (8b)$$

For simulations of the atmospheric boundary layer, where horizontal directions can typically be assumed to be homogeneous, the filtering operation is applied only in the horizontal directions, and C is assumed to be independent of the homogeneous directions and taken out of the filtering operator. Ghosal et al. (1995) presented a justification for this practice, and also

developed a localized version of the dynamic procedure for flows without any homogeneous directions. Eq. 7 is then rearranged to the following form

$$L_{ij} - \frac{1}{3}\delta_{ij}L_{kk} = CM_{ij}, \quad (9)$$

where

$$M_{ij} = \alpha_{ij} - \hat{\beta}_{ij}. \quad (10)$$

Following the method described in Lilly (1992), the coefficient C is computed so as to minimize the sum of the squares of the residuals of Eq. 9. The numerator and the denominator are averaged over the horizontal (x, y)-plane giving

$$C(z, t) = \frac{\langle M_{ij}L_{ij} \rangle_{xy}}{\langle M_{kl}M_{kl} \rangle_{xy}}. \quad (11)$$

Once C is calculated, the subgrid-scale stress tensor, given in Eq. 3 is computed. As discussed above, numerical resolutions used in atmospheric flow simulations are typically too coarse to resolve a major fraction of the energetic scales in the vicinity of the surface. Near-surface models are one of the approaches that can be employed to parameterize SGS turbulent stresses in this region. We consider three near-surface models, and provide a brief explanation of each in the following sections. We note that for two of the near-surface models (canopy stress and hybrid RANS/LES model) we use a dynamic SGS model, while for the Mason–Thomson model, we use a non-dynamic Smagorinsky SGS model.

3.1 Mason and Thomson Model

In this near-surface model, the length scale in the original Smagorinsky SGS model is matched to the distance to the surface via an empirical blending function. Mason and Thomson (1992) have suggested the following form for the modified length scale:

$$\frac{1}{(l^*)^2} = \frac{1}{(C_s\Delta)^2} + \frac{1}{(\kappa z)^2}, \quad (12)$$

where κ is the von Karman constant with a value of 0.41, and z is the distance from the surface. Turbulent stresses are then computed as

$$\tau_{ij} = -2(l^*)^2|\bar{S}|\bar{S}_{ij}. \quad (13)$$

This model cannot be used in conjunction with the dynamic Smagorinsky model because the filter width Δ appears explicitly within the equations used to compute C in the dynamic procedure. Instead we have chosen to test the Mason–Thomson model in conjunction with the original non-dynamic Smagorinsky model. Mason and Thomson (1992) have also proposed a stochastic backscatter model along with the modified length scale model. The Mason–Thomson length scale model has been adopted in different studies with and without the backscatter model (Hobson et al. 1999; Mason and Brown 1999; Mason 1994). In the present study, we employ the Mason–Thomson model without the backscatter model.

3.2 Canopy Stress Model

Canopy models were originally proposed to parameterize the structure of the flow within a vegetative or structural canopy. Brown et al. (2001), however, suggested that they might also be used as near-surface models in large-eddy simulations to overcome problems associated with under-resolution close to any rough surface. Cederwall (2002), Chow et al. (2005) and

Kirkpatrick et al. (2006) have used the canopy model of Brown et al. (2001) for this purpose. In the present study, we follow the implementation of Kirkpatrick et al. (2006).

Canopy stresses near the surface are formulated as

$$\tau_{i3} = - \int_0^{h_c} C_d \cos^3 \left(\frac{\pi z}{2h_c} \right) |\bar{\mathbf{u}}| \bar{u}_i dz, \quad (14)$$

where C_d is the canopy density in m^{-1} units. Brown et al. (2001) prescribe this quantity, whereas in the present study this coefficient is calculated dynamically, such that the total stress at the first grid point above the wall is equal to the local wall shear stress u_*^2 . This is consistent with the fact that, when the dynamic Smagorinsky model is used, both resolved and SGS shear stresses approach zero at the surface (Kirkpatrick et al. 2006). The canopy model is effective over a height h_c , which is defined to be twice the filter size at the first grid point above the surface $(2(dx \cdot dy \cdot dz_1)^{1/3})$. Canopy stresses are added onto the SGS turbulent stresses that are modelled using the dynamic Smagorinsky model. We stress that the canopy model does not imply any sort of canopy—vegetative, structural, or otherwise—and the so-called canopy stress model is simply a computational scheme to represent stresses near rough surfaces for a class of SGS models that would otherwise fail in this region.

3.3 Hybrid RANS/LES model

Surface stress boundary conditions given in Eq. 2 were derived to be consistent with the mean logarithmic wind profile, for which the implied length scale is the distance from the surface. The length scale in the LES SGS model is the filter width, and close to the surface this definition may not be compatible with the implied length scale in the surface stress boundary condition, which is the distance to the surface. To address this compatibility issue, we employ a mixing length based RANS model near the surface, for which the length scale is the distance to the surface, and make a transition to the LES model at a predetermined distance above the surface. This approach was originally suggested by Sullivan et al. (1994). The present model differs from the model of Sullivan et al. (1994) in terms of the LES SGS model and the details of transition from RANS to LES. In fact, our formulation is closer to the length scale blending approach of Mason and Thomson (1992). The present model, however, also differs from the Mason-Thomson model by generating an ensemble-averaged field in the vicinity of the surface, as will be demonstrated in the results section below.

It can be shown analytically that the logarithmic wind profile can be derived from the following eddy viscosity definition (Panofsky and Dutton 1984)

$$\nu_t = \kappa u_* z, \quad (15)$$

where u_* is the friction velocity defined as $\sqrt{\tau_{sfc}}$ with τ_{sfc} being the surface shear stress. The above form is also identical to the following definition

$$\nu_t = (\kappa z)^2 \frac{\partial U}{\partial z}, \quad (16)$$

which is the well-known mixing length model of Prandtl (1925). Here, U is the magnitude of the velocity. In our hybrid RANS/LES formulation, we use the length scale in the above definition close to the surface. This effectively guarantees a logarithmic wind profile. Away from the surface our model makes a transition to the length scale computed by the dynamic Smagorinsky model using a blending function. Following the suggestion of van Driest (1956) an exponential form is selected as the empirical blending function,

$$\nu_t = [(1 - \exp(-z/h))^2 (C\Delta^2) + \exp(-z/h)^2 (\kappa z)^2] |S|. \quad (17)$$

Here, h is the altitude controlling the transition from the RANS to the LES formulation. In the above formulation, the dynamic coefficient C is calculated using the procedure described in Eqs 3–11. For the purpose of simplicity, the blended eddy viscosity given in Eq. 17 is not considered within the dynamic procedure, because, in the vicinity of the surface, the contribution from the mixing length model dominates the eddy viscosity formulation through the exponential blending function

In order to aid the selection of h prior to a simulation, we first determine the bounds on h . The upper bound on h can be calculated following the rule of thumb that a logarithmic wind speed profile is expected within the surface layer, which is roughly the bottom 10 percent of the atmospheric boundary layer (Stull 1988; Panofsky 1974). The height of the atmospheric boundary layer (h_{ABL}) depends on stability conditions. A single formula that is valid for all stability conditions is not available. Using dimensional arguments, however, an approximation can still be made as

$$h_{ABL} \approx Cu_*/f, \quad (18)$$

where values of 0.15–0.35 have been reported for the constant of proportionality C (Panofsky and Dutton 1984; Andren et al. 1994). Based on this approximation and other numerical studies of the neutrally stratified atmospheric boundary layer (Andren et al. 1994; Kosovic 1997; Panofsky 1974), in the present study (in which $u_* \simeq 0.42 \text{ m s}^{-1}$ and $f = 10^{-4} \text{ s}^{-1}$) we define $h_{ABL} = 1500 \text{ m}$, and consider the surface layer height to be 150 m. We note that these values are specific to the current simulation problem.

The value of the lower bound on h depends on the spatial resolution adopted for the simulation. In LES, the spatial resolution becomes an integral part of the SGS model through the filter width. Hence, it is essential to provide a resolution that can resolve the energetic scales. Within the surface layer, the characteristic size of the large energetic eddies scales with the distance to the surface. Furthermore, the Nyquist theorem states that the resolution should be at least half the size of the wavelength in order to represent a waveform numerically (Stull 1988). Using these two points we define a parameter γ for the spatial resolution as

$$\gamma = \frac{z}{(2\Delta)}, \quad (19)$$

where z represents the physical length scale of the eddies, and Δ represents the numerical length scale imposed by the LES model. In regions where γ is less than unity, the simulation is considered to be under-resolved for energetic scales, contradicting the LES assumption that the energetic large eddies are resolved. Hence, a RANS formulation is more suitable in these regions. We note that this criterion is by no means exact. Firstly the question as to which definition of Δ gives the best representation of the size of the smallest resolvable scales on an anisotropic grid is yet to be satisfactorily resolved. Secondly, the size of the smallest scales that are actually resolved in a given simulation also depends on the numerical schemes used to discretize the equations. The formula also does not account for the effect of stratification, for which the physical length scale is not exactly the distance to the surface. Figure 1 shows the variation of the resolution parameter γ within the surface layer and also shows the under-resolution limit for two different grid resolutions, which are stretched in the vertical direction using an exponential scheme.

With the upper and lower bounds defined as above, a reasonable value for h can then be selected from the following range

$$z(\gamma = 1) < h < 0.10h_{ABL}. \quad (20)$$

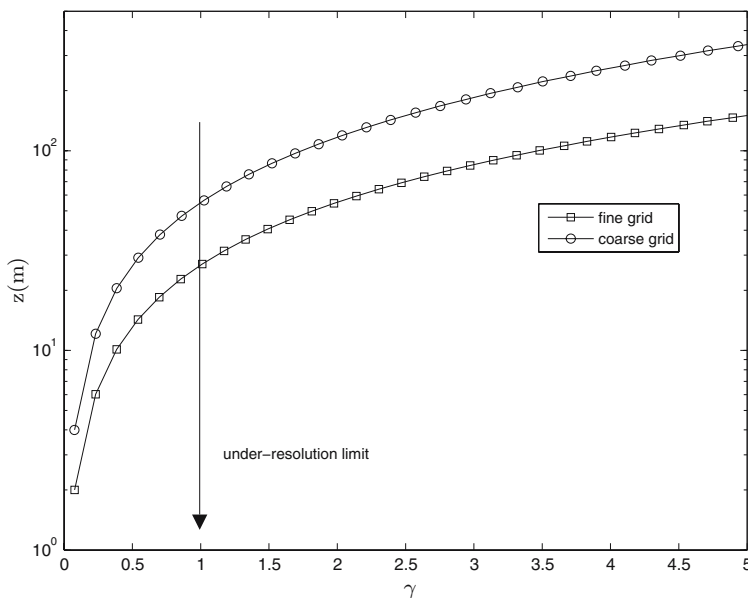


Fig. 1 Variation of the spatial resolution parameter within the surface layer for both the coarse and the fine grids, as described in Sect. 5

Based on our numerical experiments, and since we have a smooth transition from RANS to LES formulation through an exponential blending function, we suggest that h should be equal to the height where $\gamma \approx 3$, which corresponds approximately to 150 m and 75 m on the coarse and fine grids used in our study, respectively. We found a higher value for γ to be detrimental, because it tends to dampen flow structures that could otherwise be resolved.

The current model can also be extended to take into account different atmospheric stability conditions. A stability dependent form of the model is

$$\nu_t = [(1 - \exp(-z/h))^2 (C\Delta^2) + \exp(-z/h)^2 (\frac{\kappa z}{\phi_m})^2] |S|, \quad (21)$$

where ϕ_m is the dimensionless shear, and its value is unity for neutral stability. Formulae for dimensionless shear under various stability conditions are given in [Panofsky and Dutton \(1984\)](#). Since scalar quantities also exhibit logarithmic profiles within the surface layer, the current hybrid RANS/LES approach may also be used to model subgrid fluxes of scalar quantities.

We note that the present approach uses a simple mixing length model in the near-surface region, which is suitable for the present flat terrain problem but it might not be suitable for simulations of complex terrain. Hybrid RANS/LES approaches based on transport equations for turbulent kinetic energy and dissipation rate are also available in the literature, and they are generally adopted for complex geometry engineering applications (e.g. [Temmerman et al. 2005](#); [Xiao et al. 2004](#); [Abe 2005](#)).

4 Numerical schemes

Simulations were performed using the LES atmospheric research code DHARMA. The numerical methods used in DHARMA are described in detail in [Stevens and Bretherton](#)

(1996), and Stevens et al. (2000). The governing equations are integrated using a forward-in-time projection method based on a second-order Runge-Kutta scheme (Bell and Marcus 1992). The spatial discretization is performed on a staggered grid. A third-order accurate upwind-biased scheme is used for the advection terms, whereas diffusion and pressure gradient terms are discretized using second-order accurate central differencing schemes. A direct solver based on fast Fourier transform (FFT) is utilized for solving the pressure Poisson equation, and the code is parallelized to run on various platforms using the message passing interface (MPI).

5 Results and discussion

In this section, we present the results for simulations of a neutrally stratified atmospheric boundary layer. We chose our computational parameters following the study of Andren et al. (1994) with few adaptations. The computational domain size is $3000\text{ m} \times 1500\text{ m} \times 1500\text{ m}$. Simulations are performed on two grids in order to evaluate the effect of spatial resolution on the results. The *coarse grid* has a spatial resolution of $64 \times 32 \times 64$ points, and the *fine grid* has a spatial resolution of $128 \times 64 \times 128$ in the x , y , and z directions, respectively. The average filter width Δ is thus 18.6 m and 37.2 m for the fine and coarse grids, respectively. In the vertical direction, the grid points are clustered near the surface using an exponential distribution extending up to the top boundary. The first grid point for the horizontal component of the velocity is located 4 m from the surface in the coarse grid and 2 m in the fine grid. Apart from the resolution and parameter sensitivity results, all our results are produced using the fine grid. The flow is driven by a large-scale pressure gradient that would balance a 10 m s^{-1} geostrophic wind in the x direction. The Coriolis parameter is set to 10^{-4} s^{-1} , and the roughness parameter z_0 has a value of 0.1 m. A dimensionless time unit can be defined based on the Coriolis parameter ($1/f$). The simulations were run over a period of $10\text{ }f^{-1}$ with a variable timestep calculated such to ensure that the advective and diffusive stability criteria of the numerical scheme are satisfied. The statistics are collected during the final $4\text{ }f^{-1}$ of the simulation. Time evolution of the friction velocity u_* is plotted in Fig. 2. As seen from this figure, statistics remain fairly stationary during the averaging period. Ensemble averaged quantities are obtained by collecting data every $6 \times 10^{-3}\text{ }f^{-1}$, which corresponds to 60 s, and averaging them both in time and in horizontal space. Ensemble averaged quantities are indicated with the symbol $\langle \rangle$.

Figure 3 demonstrates the sensitivity of the hybrid RANS/LES model to spatial resolution and model parameter h . The value of h is varied systematically and the results progressively deviate from the logarithmic wind speed profile as h decreases. When the grid spacing is halved in each direction, however, the sensitivity to h diminishes giving closer agreement with the log-law. Following our guidance on the selection of the model parameter h , it appears that $h = 150\text{ m}$ and $h = 75\text{ m}$ can be adopted to get good agreements with the log-law on the coarse and fine grids, respectively. The contour plots of the wind speed in Fig. 4, show more detailed flow structures on the fine grid as compared with the coarse grid. The influence of the model parameter h on the flow dynamics is also apparent in Fig. 4. The smooth, layered zone within the surface layer is due to the ensemble-averaging effect of the RANS model. The thickness of this zone is controlled mainly by the parameter h . As can be seen in Fig. 4, however, this relationship is somewhat non-linear. For $h = 150\text{ m}$ the top of the smooth zone lies at a height of approximately 300 m, whereas when h is decreased by half the top of the smooth zone is reduced to approximately 100 m.

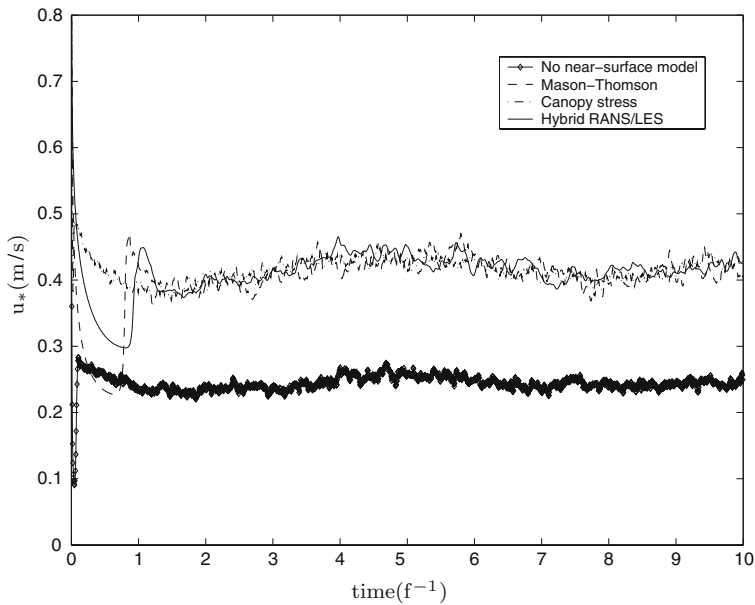


Fig. 2 Time series of the friction velocity using the fine grid. $h = 75$ m is used in the hybrid RANS/LES model

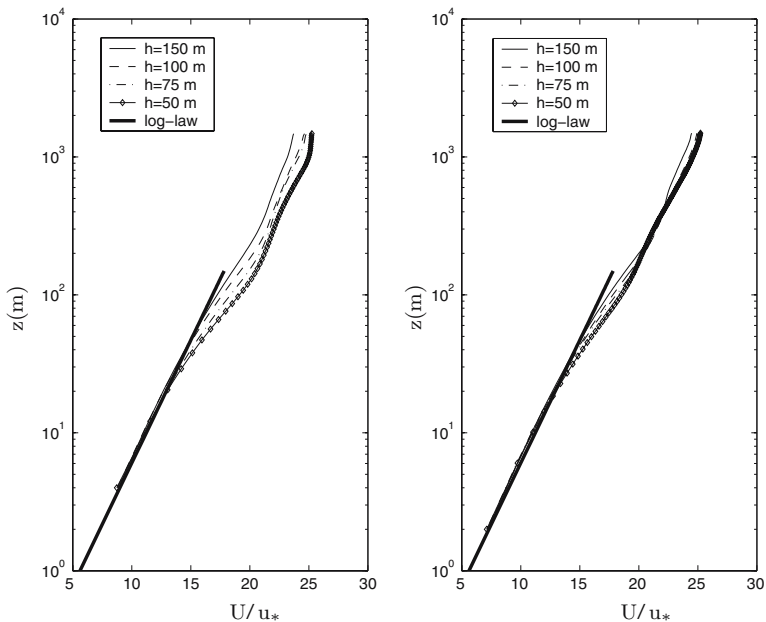


Fig. 3 Spatial resolution and model parameter (h) sensitivities of the normalized mean wind speed profile produced by the hybrid RANS/LES model. Coarse grid ($64 \times 32 \times 64$) and fine grid ($128 \times 64 \times 128$) results are presented on the left and right panels, respectively

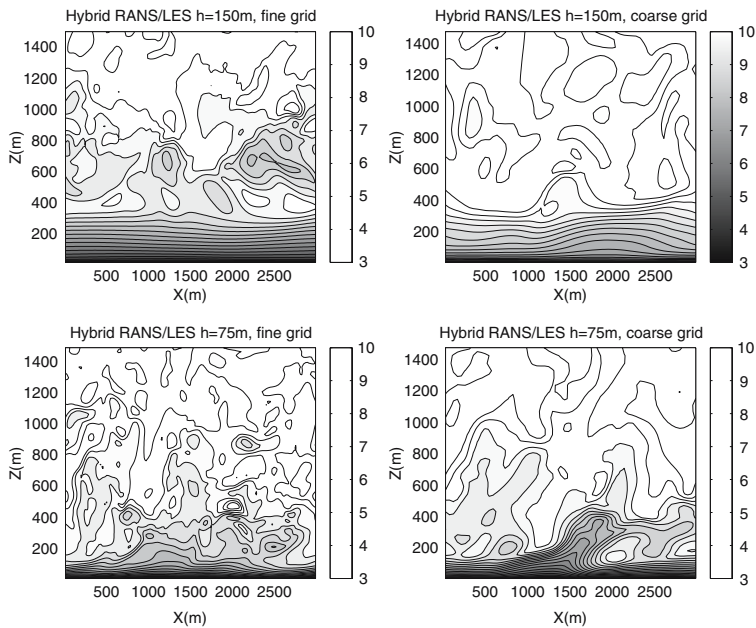


Fig. 4 Contours of the instantaneous wind speed plotted on the $x - z$ plane at $y = 750$ m and at time 10^{-1}

Agreement with the logarithmic wind speed profile is a standard measure of SGS model performance in the surface layer. [Andren et al. \(1994\)](#) compared simulations of a neutrally stratified atmospheric boundary layer using different LES codes. They concluded that results were most sensitive to the SGS model in the lower third of the boundary layer, and that commonly used SGS models failed to reproduce the logarithmic wind speed profile in the vicinity of the surface. Figure 5 shows a comparison of the mean wind speed profiles on both the fine and coarse grids for all the models considered in the present study. The dynamic Smagorinsky model without a near-surface model produces an erroneous profile, and the results do not improve when the grid is refined. This result confirms the findings of [Cabot et al. \(1999\)](#) that providing only the surface stress boundary condition is not sufficient to model the unresolved turbulent motions close to a surface. The erroneous profile is not surprising. As discussed above, the underlying assumptions of the LES formulation are not satisfied in poorly resolved regions of the flow. For both the coarse and the fine grids used in the present study, these regions occupy a substantial volume within the surface-layer domain, as was shown in Fig. 1.

The near-surface models considered in the present study, namely, the Mason–Thomson model, the canopy stress model and the hybrid RANS/LES model, have been developed specifically to parameterize the unresolved scales near the surface. The canopy stress model and the hybrid RANS/LES model use the dynamic Smagorinsky model away from the surface, whereas the Mason–Thomson model uses the original Smagorinsky model. As seen in Fig. 5, results of all simulations using near-surface models are much closer to the logarithmic wind speed profile than the results without a near-surface model. However, noticeable differences exist among them. We judge the three models based on how close they are to the log-law and how high they can maintain a logarithmic profile within the surface layer. Clearly, the closest agreement with the log-law is achieved with the hybrid RANS/LES model. This is due to

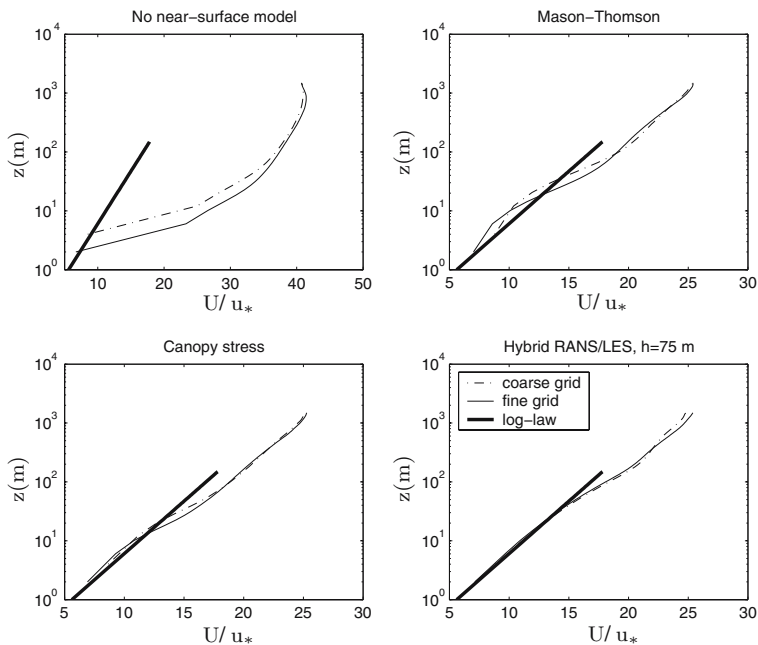


Fig. 5 Comparison of the mean wind speed profile using different models and spatial resolutions

the fact that the length scale in the RANS eddy viscosity is taken to be the distance from the surface, which can be shown analytically to give a log-law velocity profile. We may also observe from the results of the hybrid RANS/LES model that the sensitivity to the resolution parameter γ is not significant for values close to our suggested value (≈ 3). For instance, for $h = 75$ m, γ has a value of ≈ 1.5 on the coarse grid, and it has a value of ≈ 3 on the fine grid.

The canopy stress model, by design, augmentates the turbulent stresses up to a height of $2\Delta_1$, twice the filter size at the first grid point above the surface, which corresponds to 26 m and 52 m on the fine and coarse grids, respectively. As Fig. 5 shows, it does a good job of producing the logarithmic wind speed profile up to these heights.

Figure 6 presents isosurfaces of the spanwise component of the instantaneous vorticity field. The impact of adopting any of the near-surface models can be seen in the richness of the flow structures and their existence beyond the surface layer. Figure 7 shows notable differences in the corresponding resolved velocity variances. The profiles are roughly the same above ≈ 400 m for all the models except dynamic Smagorinsky without a near-surface model. Within the surface layer, the resolved velocity variances in the hybrid model simulation are damped due to the ensemble-averaged modeling assumption in that region. As seen from Figs. 6 and 7, the simulations using the canopy stress and the Mason-Thomson models are able to accommodate more resolved turbulence compared with the hybrid model. Such abundance of flow structures creates high turbulence stresses, as is evident in Fig. 8. This difference can be important, for instance, in the study of plume transport, because the level of turbulence plays a role in the plume spread in vertical and horizontal directions. Recent studies (Drobinski et al. 2004; Hogstrom et al. 2002) on the structure of a near-neutral atmospheric boundary layer argue that detached eddies formed above the surface-layer contribute

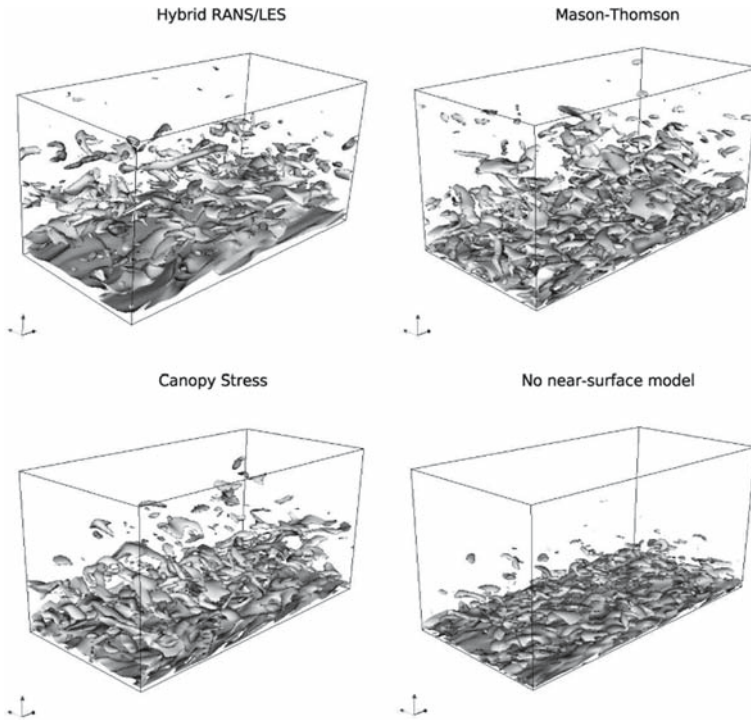


Fig. 6 Visualization and comparison of spanwise component of the instantaneous vorticity fields within the full domain. The results at time $10 f^{-1}$ are shown. $h = 75$ m is used in the hybrid RANS/LES model

to the surface-layer turbulence by penetrating deep into the surface layer and impinging on the surface. Due to their ability to resolve turbulence down to a considerably lower level, the canopy stress and Mason-Thomson model would be better able to capture these effects.

The streamwise and spanwise components of the total and resolved stress profiles are compared in Figs. 8 and 9, respectively. By total stress, we mean the resolved turbulent stresses plus the modeled SGS turbulent stresses. As can be seen from these plots, simulations with near-surface models produce similar profiles. Without a near-surface model, however, the dynamic Smagorinsky model gives insufficient SGS dissipation, and predicts a quite different profile for the total turbulent stress. It also produces substantial wiggles close to the surface. These wiggles are a result of kinetic energy accumulation near the surface, which can also be seen in the resolved velocity variances shown in Fig. 7. The friction velocity is also significantly underpredicted when no near-surface model is used. The fact that the results of the three remaining models are so close to each other is not surprising. As can be seen in Fig. 2, all three models produce very similar values of the friction velocity. We therefore expect the stress profiles to be similar, since, in the limit of infinite Rossby number, the normalized total stresses are universal functions of zf/u_* . (Garraff 1992)

The resolved turbulent stresses are also shown in the right hand panels of Figures 8 and 9. Within the lower 100 m of the boundary layer, a large range of turbulent scales are modelled with the hybrid RANS/LES model, whereas other surface models are effective only within the lower 50 m of the boundary layer. The extent of RANS modelling in the hybrid RANS/LES model is controlled through the value of h in Eq. 17. We provided guidance to

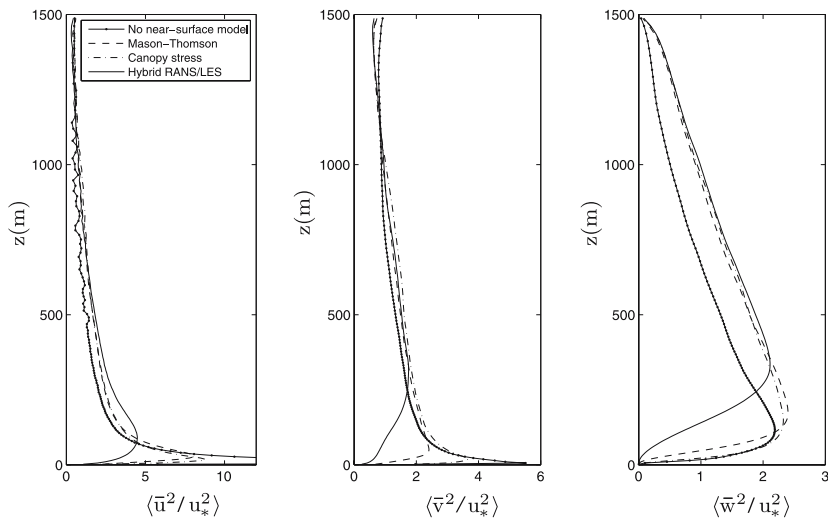


Fig. 7 Comparison of the resolved velocity variances. $h = 75$ m is used in the hybrid RANS/LES model

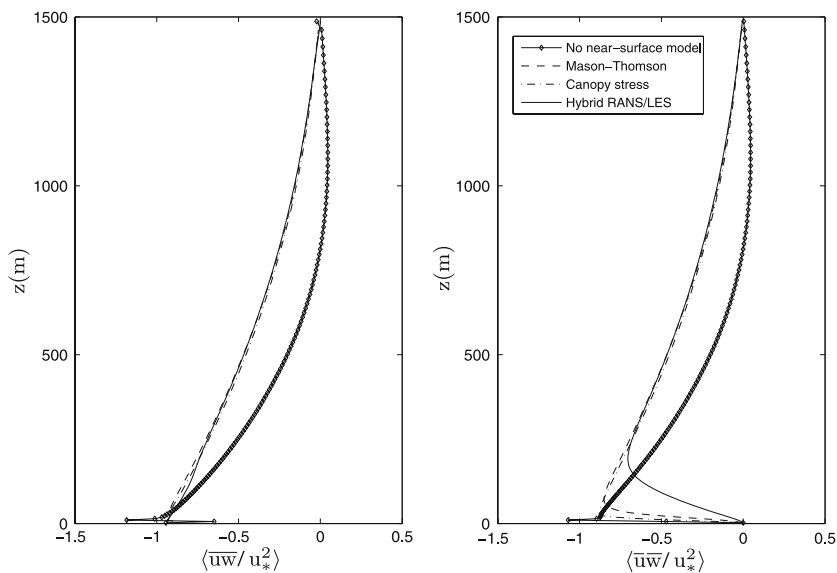


Fig. 8 Comparison of streamwise component of the mean total (left) and resolved (right) stress. $h = 75$ m is used in the hybrid RANS/LES model

selecting an appropriate value for h in Sect. 3.3 and studied the sensitivity of h on the mean wind speed in Fig. 3

Figure 10 shows the normalized energy spectra of streamwise velocity at altitudes of $z = 100$ m and $z = 1000$ m. With no near-surface model, the peak in the spectrum is much lower compared with the other three models at both altitudes, because, as was discussed above, without a near-surface model, the LES significantly underpredicts the friction velocity. The

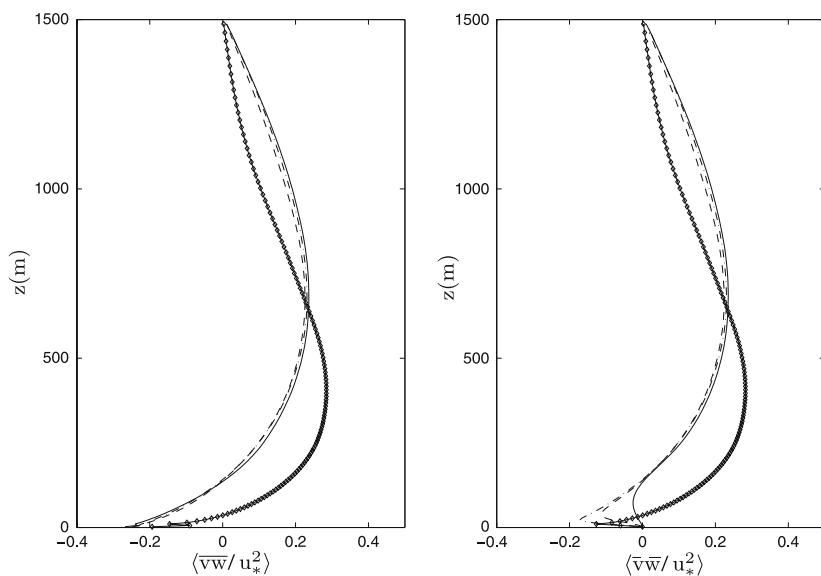


Fig. 9 Comparison of spanwise component of the mean total (left) and resolved (right) stress. $h = 75$ m is used in the hybrid RANS/LES model. Line patterns as in Fig. 8

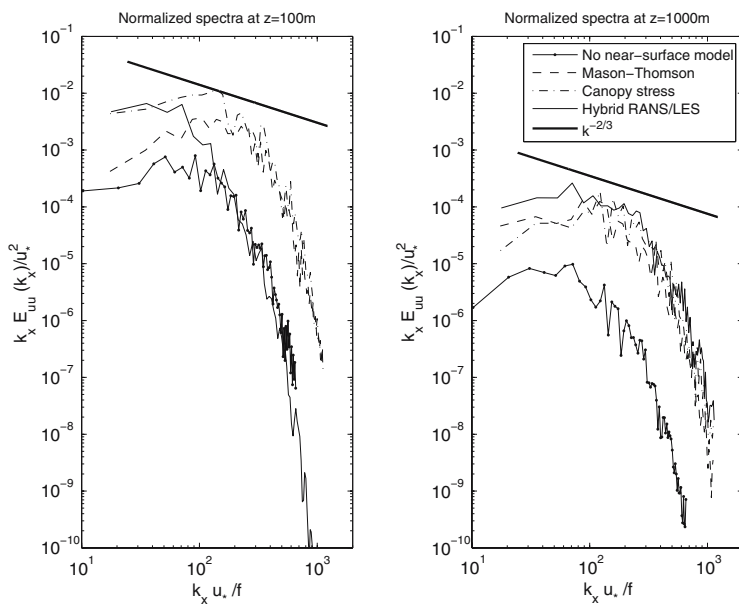


Fig. 10 Normalized energy spectra of streamwise velocity. Plots on the left and right hand side show spectra at $z = 100$ m and $z = 1000$ m, respectively. $h = 75$ m is used in the hybrid RANS/LES model

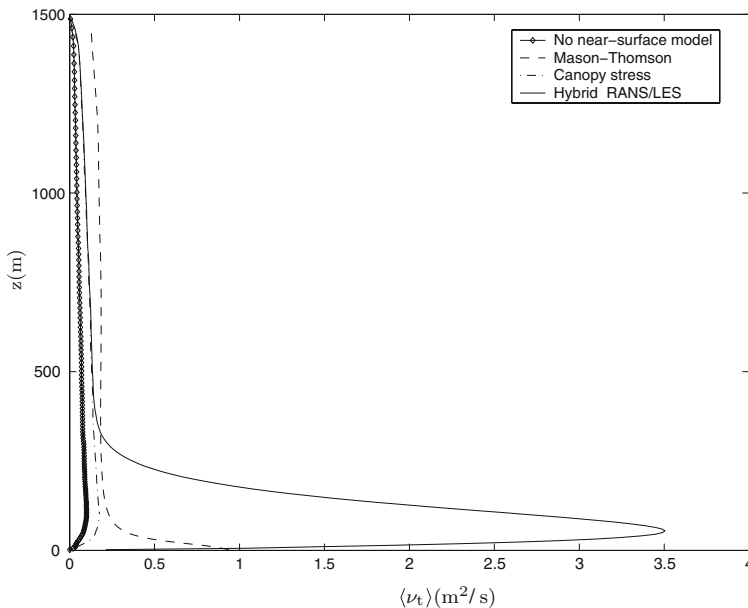


Fig. 11 Comparison of the mean SGS viscosity profiles. $h = 75$ m is used in the hybrid RANS/LES model

spectrum at an altitude of $z = 100$ m demonstrates the effect of the hybrid RANS/LES model in the vicinity of the surface. The spectrum decays rapidly from the peak level, because the dissipation of the hybrid model acts over a wide range of wavenumbers, thus giving what is essentially an ensemble-averaged velocity field. The spectra at $z = 1000$ m, however, are similar for all the three simulations using near-surface models. We note that our simulations predict a narrower inertial sub-range than expected, which is a well-known issue with upwind biased advection schemes.

We present turbulent eddy viscosity profiles in Fig. 11. Away from the surface, nearly identical profiles are obtained with the hybrid RANS/LES model and the canopy stress model, which is expected, because both models adopt the dynamic Smagorinsky model in that region. However, both of the models produce higher eddy viscosity levels above the surface layer as compared to the dynamic Smagorinsky model without a near-surface model. Near the surface, the eddy viscosity levels are much lower with the canopy stress model, because the model directly modifies the turbulent stress terms but not the eddy viscosity term. On the other hand, the eddy viscosity produced by the hybrid RANS/LES model is much greater in the vicinity of the surface. With a high level of eddy viscosity, turbulent motions near the surface are dampened, and the resulting flow field variables can be considered as ensemble-averaged quantities. It is also important to note that a high eddy viscosity level imposes diffusive stability limits on the timestep size when the momentum equations are discretized explicitly. Among all models, the Mason-Thomson predicts higher levels of eddy viscosity above the surface layer, because it adopts the original Smagorinsky model there.

Finally, in Fig. 12 we compare the dynamically computed model coefficients ($C_s = \sqrt{C}$) occurring in simulations using the hybrid RANS/LES model, canopy stress model and no near-surface model. The model coefficients are very close to each other above the surface layer, and they are within the typical range of the model coefficient (0.10–0.20) used in the standard Smagorinsky model. The hybrid RANS/LES model produces an ensemble-averaged

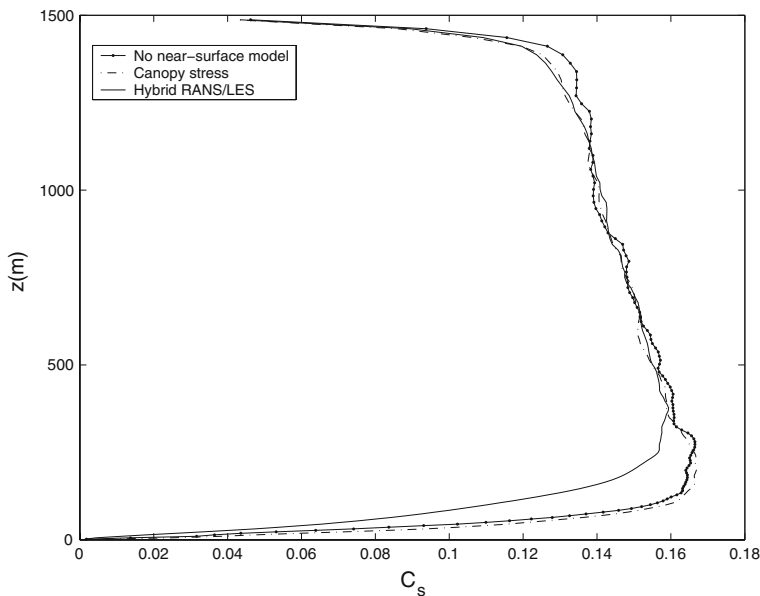


Fig. 12 Comparison of dynamically computed SGS model coefficients. $h = 75$ m is used in the hybrid RANS/LES model

field in the vicinity of the surface with lower levels of resolved turbulence. As can be seen from Fig. 12, the dynamic model coefficient adapts itself to this change in the flow structure, but the net effect of this behaviour on the eddy viscosity is not significant, because the contributions from the mixing length RANS model are dominant due to exponential blending between two models, which is also evident in the eddy viscosity distributions given in Fig. 11.

6 Conclusions

Numerical resolutions that are typically used in atmospheric boundary-layer simulations are insufficient to resolve a large fraction of the energetic scales within the surface layer. One of the strategies to address this issue is to use a near-surface model that parameterizes the unresolved scales of the turbulent flow. In this study, we have presented results for large-eddy simulations of a neutrally stratified atmospheric boundary layer using both dynamic and non-dynamic eddy viscosity models. In particular, we have investigated the performance of different near-surface models in predicting the mean flow field at different grid resolutions. We considered the near-surface models of [Mason and Thomson \(1992\)](#) and [Brown et al. \(2001\)](#) as well as a hybrid RANS/LES model, which is a combination of Prandtl's mixing length model and the dynamic Smagorinsky model. We have also provided an extension of the hybrid RANS/LES model to take into account different stability conditions.

Our simulations demonstrate that, if a large fraction of energetic scales in the surface layer cannot be resolved, then using a near-surface model in conjunction with the SGS model greatly enhances the predictions. Of the near-surface models considered, the hybrid RANS/LES model gave the closest agreement with the theoretical logarithmic wind speed profile. The

prescribed parameter h in the hybrid model controls the transition from RANS to LES modeling. We systematically varied this parameter and showed that the logarithmic wind speed profile can be reproduced, and sensitivity to the parameter h noticeably diminishes with increased spatial resolution. We determined the bounds on the value of this parameter and offered guidance for its selection in the form of a formula based on the spatial resolution, which can be evaluated prior to the simulations. The hybrid model was found to produce an ensemble averaged velocity field close to the surface by suppressing the turbulent motions in this region that could otherwise be resolved numerically to a certain degree. The canopy stress and Mason-Thomson models were found also to give good agreement with the log-law, while explicitly resolving more of the turbulence in the surface layer, which can be advantageous in the studies of eddies within in the surface layer.

References

- Abe K (2005) A hybrid LES/RANS approach using an anisotropy-resolving algebraic turbulence model. *Int. J Heat Fluid Flow* 26:204–222
- Andren A, Brown AR, Graf J, Mason PJ, Moeng C-H, Nieuwstadt FTM, Schuman U (1994) Large-eddy simulation of a neutrally stratified boundary layer: A comparison of four computer codes. *Quart J Roy Meteorol Soc* 120:1457–1484
- Balaras E, Benocci C, Piomelli U (1996) Two-layer approximate boundary conditions for large-eddy simulation.. *AIAA J*. 34:1111–1119
- Bell JB, Marcus DL (1992) A second-order projection method for variable-density flows. *J Comput Phys* 101: 334–348
- Bohnert M (1993) A numerical investigation of cloud-topped planetary boundary layers. Ph.D. thesis, Stanford University
- Brown AR, Hobson JM, Wood N (2001) Large-eddy simulation of neutral turbulent flow over rough sinusoidal ridges. *Boundary-Layer Meteorol* 98:411–441
- Cabot W (1997) Wall models in large-eddy simulation of separated flow. *Annual Research Briefs, Center for Turbulence Research, NASA-Ames/Stanford University*, 97–106.
- Cabot W, Moin P (2000) Approximate wall boundary conditions in the large-eddy simulation of high Reynolds number flow. *Flow Turbul Combust* 63:269–291
- Cabot W, Jimenez J, Baggett JS (1999) On wakes and near-wall behavior in coarse large-eddy simulation of channel flow with wall models and second-order finite difference methods. *Annual research briefs, Center for Turbulence Research, NASA-Ames/Stanford University*, pp 343–354
- Cederwall RT (2002) Large-eddy simulation of the evolving stable boundary layer over flat terrain. Ph.D. thesis, Stanford University, 231 pp
- Chow FK, Street RL, Xue M, Ferziger JH (2005) Explicit filtering and reconstruction turbulence modeling for large eddy simulation of neutral boundary layer flow. *J Atmos Sci* 62:2058–2077
- Drobinski P, Carlotti P, Newsom RK, Banta RM, Foster RC, Redelsperger J (2004) The structure of the near neutral atmospheric surface layer. *J Atmos Sci* 61:699–714
- Garratt JR (1992) *The atmospheric boundary layer*. Cambridge University Press UK, 316 pp
- Germano M, Piomelli U, Moin P, Cabot WH (1991) A dynamic subgrid-scale eddy viscosity model. *Phys Fluids* 3:1760–1765
- Ghosal S, Lund TS, Moin P, Akselvoll K (1995) A dynamic localization model for large-eddy simulation of turbulent flows. *J Fluid Mech* 286:229–255
- Hobson JM, Wood N, Brown AR (1999) Large-eddy simulations of neutrally stratified flow over surfaces with spatially varying roughness length. *Quart J Roy Meteorol Soc* 125:1937–1958
- Hogstrom U, Hunt J, Smedman A-S (2002) Theory and measurements for turbulence spectra and variances in the atmospheric neutral surface layer. *Boundary-Layer Meteorol* 103:101–124
- Kirkpatrick MP, Ackerman AS, Stevens DE, Mansour NN (2006) On the application of the dynamic Smagorinsky model to large-eddy simulations of the cloud-topped atmospheric boundary layer. *J Atmos Sci* 63:526–546
- Kosovic B (1997) Subgrid-scale modelling for the large-eddy simulation of high-Reynolds number boundary layers. *J Fluid Mech* 336:151–182
- Lilly DK (1992) A proposed modification of the Germano subgrid-scale closure method. *Phys Fluids* 4:633–635

- Mason PJ (1994) Large-eddy simulation: A critical review of the technique. *Quart J Roy Meteorol Soc* 120: 1–26
- Mason PJ, Brown AR (1999) On subgrid models and filter operations in large eddy simulation. *J Atmos Sci* 56:2101–2114
- Mason P, Callen N (1986) On the magnitude of the subgrid-scale eddy coefficient in large-eddy simulations of turbulent channel flow. *J Fluid Mech* 162:439–462
- Mason P, Thomson D (1992) Stochastic backscatter in large-eddy simulations of boundary layers. *J Fluid Mech* 242:51–78
- Moeng CH (1984) A large-eddy simulation model for the study of planetary boundary layer turbulence. *J Atmos Sci* 41:2052–2062
- Panofsky HA (1974) The atmospheric boundary layer below 150 meters. *Annu Rev Fluid Mech* 6:147–177
- Panofsky HA, Dutton JA (1984) *Atmospheric turbulence*. John Wiley, New York, 397 pp
- Porte-Agel F, Meneveau C, Parlange MB (2000) A scale-dependent dynamic model for large-eddy simulation: application to a neutral atmospheric boundary layer. *J Fluid Mech* 415:261–284
- Prandtl L (1925) Bericht über die Entstehung der Turbulenz. *Z Angew Math Mech* 5:136–139
- Sagaut P (2002) *Large Eddy simulation for incompressible flows*. Springer-Verlag, Berlin, 426 pp
- Schumann U (1975) Subgrid-scale model for finite difference simulations of turbulent flows in plane channels and annuli. *J Comput Phys* 18:376–404
- Smagorinsky J (1963) General circulation experiments with the primitive equations. I. The basic experiment. *Mon Wea Rev* 91:99–164
- Stevens DE, Bretherton CS (1996) A forward-in-time advection scheme and adaptive multilevel flow solver for nearly incompressible atmospheric flow. *J Comput Phys* 129:284–295
- Stevens B, Lenschow DH (2001) Observations, experiments, and large eddy simulation. *Bull Amer Meteorol Soc* 82:283–294
- Stevens DE, Bell JB, Almgren AS, Beckner VE, Rendleman CA (2000) Small-scale processes and entrainment in a stratocumulus marine boundary layer. *J Atmos Sci* 57:567–581
- Stull RB (1988) *An introduction to boundary layer meteorology*. Kluwer Academic Publishers, Dordrecht, 666 pp
- Sullivan PP, McWilliams JC, Moeng CH (1994) A subgrid-scale model for large-eddy simulation of planetary boundary layer flows. *Boundary-Layer Meteorol* 71:247–276
- Sullivan PP, Horst TW, Lenschow DH, Moeng C-H, Weil JC (2003) Structure of subfilter-scale fluxes in the atmospheric surface layer with application to large-eddy simulation modelling. *J Fluid Mech* 482: 101–139
- Temmerman L, Hadziabdic M, Leschziner MA, Hanjalic K (2005) A hybrid two-layer URANS-LES approach for large eddy simulation at high Reynolds numbers. *Int J Heat Fluid Fl* 26:173–190
- vanDriest ER (1956) On turbulent flow near a wall. *J. Aero. Sci.* 23:1007–1011
- Wang M, Moin P (1992) Dynamic wall modeling for large-eddy simulation of complex turbulent flows. *Phys Fluids* 14:2043–2051
- Wyngaard JC, Peltier LJ, Khanna S (1998) LES in the surface layer: Surface fluxes, scaling, and SGS modeling. *J Atmos Sci* 55:1733
- Xiao X, Edwards JR, Hassan HA (2004) Blending functions in hybrid Large-eddy/Reynolds-Averaged Navier-Stokes simulations. *AIAA J.* 42:2508–2515